NANO LETTERS

2006
Vol. 6, No. 8
1663−1668

Transmission Electron Microscopy Study of Individual Carbon Nanotube Breakdown Caused by Joule Heating in Air

Kristian Mølhave,*,† Sven Bjarke Gudnason,† Anders Tegtmeier Pedersen,† Casper Hyttel Clausen,† Andy Horsewell,‡ and Peter Bøggild†

NanoDTU, Department of Micro and Nanotechnology (MIC) and Department of Manufacturing Engineering and Management (IPL), Technical University of Denmark, DK-2800 Kgs. Lyngby, Denmark

Received April 11, 2006; Revised Manuscript Received June 15, 2006

ABSTRACT

We present repeated structural and electrical measurements on individual multiwalled carbon nanotubes, alternating between electrical measurements under ambient conditions and transmission electron microscopy (TEM). The multiwalled carbon nanotubes made by chemical vapor deposition were manipulated onto cantilever electrodes extending from a specially designed microfabricated chip. Repeated TEM investigations were then made of the progressive destruction of the nanotube structure induced by Joule heating in air. The electrical measurements indicate that the studied nanotubes behave as diffusive conductors with remarkably predictable electrical properties despite extensive structural damage.

1. Introduction. Carbon nanotubes have long been regarded as suitable candidates for active and passive components in future electronic devices. Both single-walled (SWNT) and multiwalled (MWNT) carbon nanotubes have been investigated for many such applications. The MWNTs used for the majority of electrical measurements reported in the literature have been fabricated by arc discharge (A-MWNT),[1−3] and such nanotubes are known to have a much lower defect density than carbon nanotubes fabricated with chemical vapor deposition (CVD), C-MWNT, which are typically regarded as diffusive conductors.[4,5] Defects can be of a variety of types, such as pentagon−heptagon pairs (Stone-Walls defect), vacancies and domains of graphite, corrugations, bamboo-like walls, and residues of catalysis particles.[6] However, from a practical perspective, the C-MWNTs are interesting, since they can easily be integrated in microsystems by methods such as CVD or plasma-enhanced CVD (PECVD) from prepositioned catalytic particles,[7−9] while A-MWNTs needs to be integrated into microsystems from liquid dispersions of the nanotube powder or by similar methods with little control over the placement of the individual nanotube. Despite the high defect density, C-MWNTs are also promising for electrical devices and have been shown to sustain high current densities above 10^7 A/cm^2.[10] In addition, high-density (10^{11} cm^2) transistor arrays have been made with highly defective C-MWNTs.[11]

Recently, transmission electron microscopy (TEM) compatible chips have received increased attention, as TEM allows detailed study of the structure of nanodevices. To create nanodevices accessible to the TEM electron beam, various methods have been used, such as lithographically defined contacts to nanotubes dispersed on a TEM transparent silicon nitride thin film,[12,13] or direct CVD growth of nanotubes or peapods in slits etched into chips.[14,15] The underlying substrate of planar devices has also been etched out to leave the planar nanostructure freely suspended for TEM inspection.[16] Earlier work has used a focused ion beam to mill slits for creation of individual devices for TEM investigation.[17]

In this paper, repeated TEM measurements are used to investigate how C-MWNTs change under repeated Joule heating in air to study the durability of these nanoscale structures under conditions likely to be encountered in high power devices in an ambient environment, such as interconnects in computer chips.[9]

To perform such an investigation on individual nanotubes, we have developed microfabricated cantilever chips adapted to be mounted in a TEM specimen holder. Combined electrical and TEM characterization is done by manipulating

* Corresponding author. E-mail: krm@mic.dtu.dk.
† Department of Micro and Nanotechnology.
‡ Department of Manufacturing Engineering and Management.

10.1021/nl060821n CCC: $33.50
Published on Web 07/06/2006

a nanotube to bridge two cantilever electrodes for electrical contact with the suspended part of the nanotube accessible for the TEM electron beam. In this way, we ensure that the electrical measurements are done on one specifically selected tube. Hence, suspended nanotube devices can be made without the need for chemical processing of the nanotube to create dispersions or underetching of the substrate.[16] The method also avoids using thin films for suspending the structure thus leaving the nanostructure entirely freely suspended and in pristine condition.

2. Theory. To provide a basis for understanding the Joule heating experiments, we will briefly review the conductive properties of carbon nanotubes as a function of temperature and bias voltage, as well as the oxidation effects and structural changes taking place as the nanotube is Joule heated in air.

Dai and co-workers[4] found the transport mechanism of C-MWNT to be diffusive rather than ballistic, with a resistivity of the order $10-100\ \mu\Omega$m. Although there is some variation in the current−voltage (*IV*) curves reported and in the explanations for the behavior in the literature, the *IV* measurements on C-MWNT generally show nonlinearly increasing conductance as function of low bias voltages.[10,18,19] In air, a lasting decrease of conductance will be observed if the bias voltage is increased beyond the point where a saturation effect eventually limits the current at high bias voltages in the range 1−10 V.[10,18] Oxidation of the outer shells due to Joule heating of the nanotube at the high bias voltage is mentioned as a possible explanation for the current limit. The Joule heating temperature rise at the center of the nanotube bridge, ΔT, can be estimated by solving the heat continuity equation $\kappa A T'' = -R' I^2$ for a cylindrical rod clamped at both ends with a fixed temperature,[20] giving $\Delta T = (L/(8\kappa A))P$, where L is the bridge length, A the cross-sectional area, κ the thermal conductivity and $P = UI$ the dissipated power in the bridge with bias voltage U and current I. The thermal conductivity of MWNTs has been measured to be in the wide range 25−3000 W/mK[20] and for C-MWNTs the conductivity has been found in the range 25−200 W/mK.[21,22] For a 1 μm long 100 nm diameter nanotube with a dissipated power of 1 mW, the temperature increase could be in the range 50−500 K given the wide range reported for the thermal conductivity of C-MWNTs.

The change in resistance with respect to temperature has been investigated by several groups with quite different results. To first order, the linear temperature coefficient α of resistance gives $R_2 = R_1(1 + \alpha\ \Delta T)$, where $\Delta T = T_2 - T_1$ is the temperature change. For carbon fibers, α has been measured to be in the range [−0.13;0.02] %/K.[23] For A-MWCNT, $\alpha = -0.041$%/K has been reported.[24] C-MWNT samples have also been measured to have highly linear conductance dependence on temperature $G_2 = G_1(1 + \beta\Delta T)$ in the wide range of temperatures 50−800 K,[25] while another study found both positive and negative temperature coefficients depending on the degree of disorder in the shell structure.[26] Given the wide variety of defect types and their different effects on the electrical properties of an individual nanotube shell, it seems difficult to predict the properties of an individual C-MWNT without extensive structural studies. The method presented here allows for investigations of these issues in detail on the individual nanotube.

In air, amorphous graphite begins to oxidize at around 350 °C, while carbon nanotubes generally have higher oxidation temperatures, starting around 600 °C.[27] This is often explained by the absence of dangling bonds and the protection of inner shells by the outermost one. When nanotubes are heated in air, TEM studies have shown that pits tend to form in the shell structure.[28] Oxidation occurs faster at kinks, corrugations, and at points under a state of stress due to bending.[29] In addition, when high currents are passed through a nanotube, electron scattering near defects may cause local heating effects.[30]

3. Experimental Setup. Microfabricated chips with gold-coated (10 nm Cr/100 nm Au) silicon oxide microcantilevers were made with a "O" or "U" chip shape (inset in Figure 1), adapted to fit into a standard TEM grid holder. The microfabrication process has been described previously.[31] The present work has focused on studying a C-MWNT sample produced by a ferrocene/xylene CVD process,[32] and the nanotube structure appears comparable to those used by others.[33] Individual C-MWNTs bridging the microcantilevers were positioned on the TEM chip by manipulation using a an optical microscope and a manual *xyz*-stage fitted with an etched tungsten tip. For smaller nanotubes and nanostructures, an in situ SEM manipulation setup for nanoscale resolution can be used to place the nanostructure on the cantilevers.[34]

The achieved bridge resistance was often of the order of 100 kΩ when the nanotube was initially placed on the cantilevers. Temporary condensation of water onto the chip surface resulted in a stable reduction of the bridge resistances to below 50 kΩ in about half of the investigated samples, suggesting that adhesive capillary forces pull the nanotube into close contact with the cantilever surface to provide a more stable and reliable electrical contact. The method has been used to efficiently make electrical contact to both carbon nanotubes of different types and InP nanowires.

The TEM investigation was carried out in a Philips EM 430 operating at 100 keV. Using a liquid nitrogen cooled coldfinger, low beam currents, and relatively short beam exposure times (<2 min) ensured that no significant influence on the electrical properties of the nanotubes could be attributed to the TEM observations.

The electrical measurements were made using a Keithley 2400 sourcemeter. The control program allows the voltage sweep (*IV* curve) to be paused during the experiment when predefined voltages are reached or when current saturation occurs ($dI/dV = 0$) to record the current as function of time (*It* curve) until the bias voltage sweep is continued or the experiment stopped. For convenience, conductance will be given in units of the conductance quantum, G_0, keeping in mind that the transport mechanism is not expected to be ballistic at room temperature on the μm length scales investigated here.

4. Results. A TEM image sequence of the progressive oxidation of a nanotube in air is shown in Figure 1, where

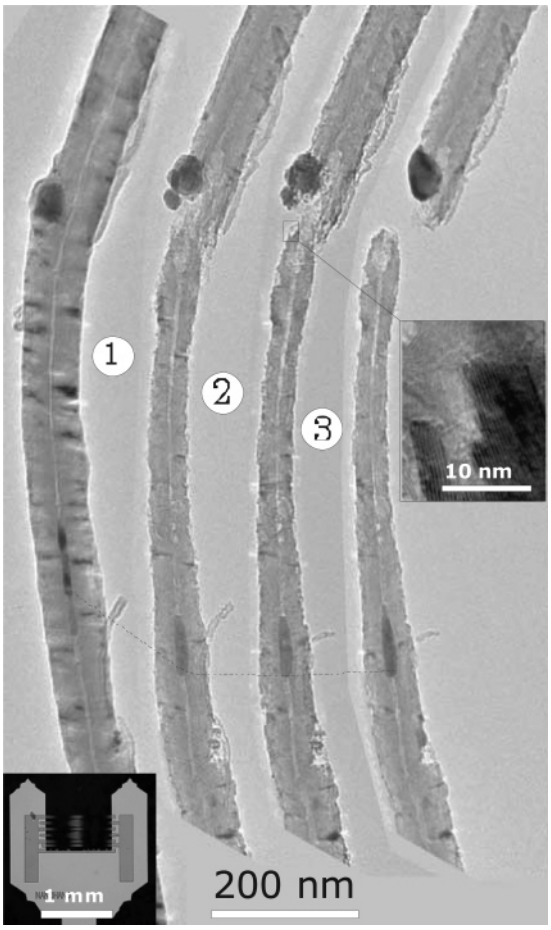

Figure 1. A series of TEM images of a C-MWNT, bridging two cantilevers on a TEM chip. The progressive destruction due to three consecutive Joule heating experiments (1−3) in air is clearly visible. The three corresponding *IV* and *It* curves recorded between the TEM images are shown in Figure 3. The dotted line indicates the motion of a catalytic particle within the nanotube central cavity. The nanotube breakdown primarily takes place in the vicinity of a particle incorporated into the shell structure, but also the middle part of the tube is considerably thinned down as a result of the Joule heating. The close-up shows the destroyed shell structure close to the catalytic particle where the termination of individual shells is clearly visible. The inset shows a U-shaped TEM compatible chip.

a Joule heating experiment has been performed between each TEM image was recorded. The nanotube clearly becomes thinner in the central part of the bridge with extensive damage in the vicinity of a large catalytic particle. The particles in the nanotube interior were generally observed to move and change shape, similar to the behavior reported by refs 33 and 35.

The C-MWNTs tested in these experiments had estimated initial cross-sectional area, A, in the range $(3-10) \times 10^3$ nm^2 (neglecting the narrow inner hole) and the length of the cantilever gap, L_{gap}, spans the range 0.7−9 μm. However, the distance between contact points of the nanotube located on top of the cantilevers, L_{tube}, may well be larger than the measured gap size as shown in the inset in Figure 2. The rough linearity of the measured resistance versus gap size indicates that this effect is only moderately important. A linear fit of the measured resistance as a function of length

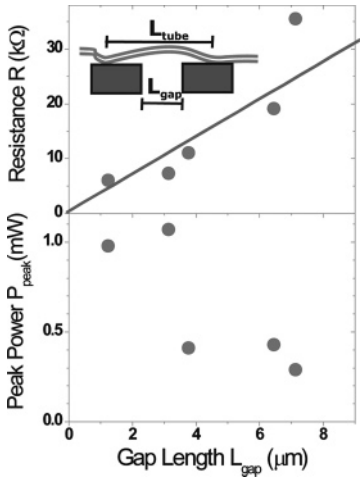

Figure 2. Overview of the electrical properties of the devices that achieved good contact to the C-MWNT (R < 50 kΩ). (a) The measured low bias resistance roughly scales with the gap length, showing that the tubes can be regarded as diffusive conductors on the micrometer scale and have a low contact resistance of the order of 0.5 kΩ. The inset illustrates that the nanotube section between contact points can be larger than the cantilever gap and that the length measurements therefore should be regarded with caution. (b) The maximum power dissipated in the bridges is around 1 mW for the shortest nanotubes and decreases with increasing gap length.

indicates an average contact resistance around 0.5 kΩ, which is less than 10% of the measured resistance for most nanotubes. The resistance through the microchip leads is only 90 Ω, hence the nanotubes may be regarded as diffusive conductors with resistance $R = \rho L/A$. The measured resistivity, ρ, is a factor 20−100 larger than the in-plane resistivity of graphite, 5×10^{-5} Ω cm[36] and thus comparable to the results by Dai et al.[4] The peak current density reaches 10^6-10^7 A/cm^2 for all nanotubes, which compares to previous studies of C-MWNT.[10] The peak power dissipated in the nanotube is quite different for the various C-MWNTs but seems to be limited to about 0.5−1 mW, as shown in Figure 2 and decreases with increasing gap length. This behavior may be expected for a heated bridging nanotube reaching the largest temperatures in the suspended part farthest away from the electrode heat sinks. All nanotubes were observed to be affected most in the middle of the gap between the electrodes, indicating that Joule heating is mainly taking place in the suspended part of the nanotube rather than at the contact points as expected for a diffusive conductor with low contact resistance.[37]

The electrical measurements on the nanotube observed in TEM in Figure 1 are shown in Figure 3 and are representative for the investigated nanotubes. Figure 3a shows the sequential *IV* curves indicated by the numbers in Figure 1. The voltage sweep was started at 0 V, and initially the sweep was stopped temporarily every 0.2 V, to observe the time dependence of the current at fixed bias, plotted in Figure 3b. As the saturation point was approached, pauses were made with smaller voltage intervals. At low bias voltages up to a bias voltage about 1.5 V, the current decay rate dI/dt is of order nA/s, which can be regarded as negligible. Above 1.5 V, dI/dt increases. Figure 3d plots the initial dI/dt at the beginning of each pause in the voltage sweep, as a function

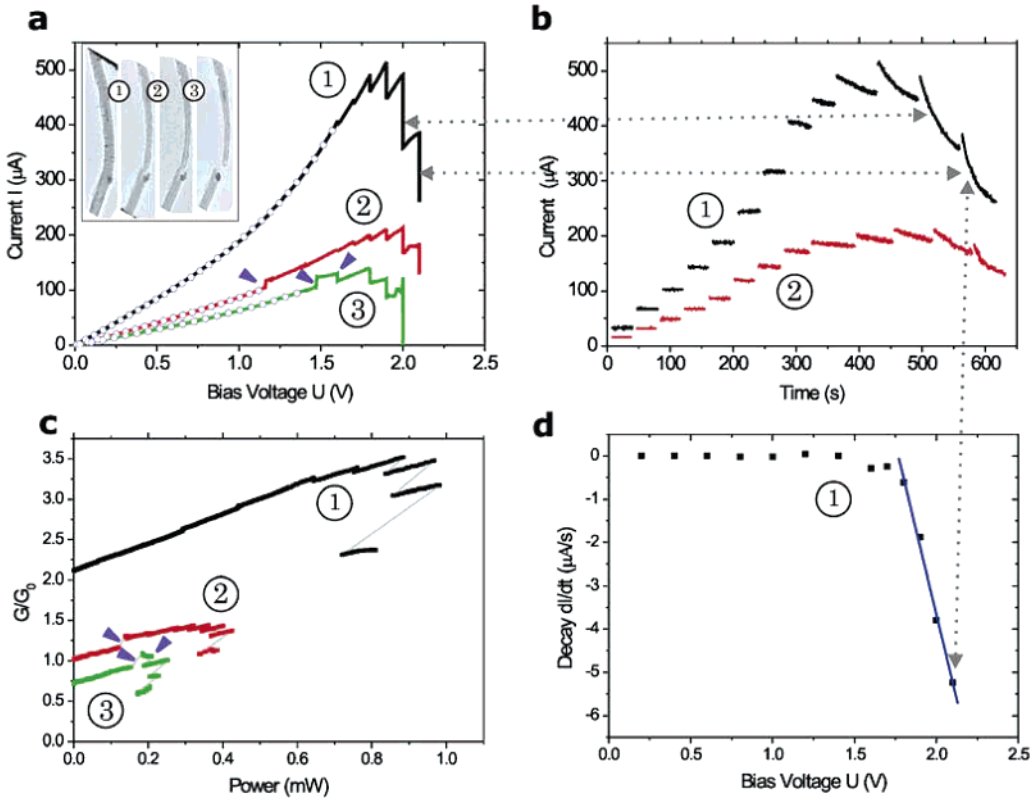

Figure 3. (a) Current through an individual C-MWNT as a function of bias voltage measured three successive times (1−3). The inset shows the TEM image sequence, also seen in Figure 1. The vertical parts of the curve appear in the intervals where the bias voltage was kept fixed, showing an increasingly strong time dependence at high bias voltages. The circles at low bias are nonlinear fits of the Joule heating IV dependence $I = U/(r + cU^2)$. (b) The current as a function of time at certain temporarily fixed bias voltages (correlations between the graphs are indicated with arrows). The current decreases faster with time above the threshold voltage, which is clear from the plot of dI/dt vs V in (d). (c) Normalized conductance G/G_0 versus dissipated power P. At fixed bias voltage, i.e., during the time sequences, the $G-P$ curve follows the gray lines ($G = P/U^2$). During the voltage sweep a dependence of the type $G = cP + 1/r$ is found for all samples with a fairly constant factor c. The small arrows in parts a and c indicate a glitch in the current source at 100 μA due to an automatic range shift.

of the fixed bias voltage. From 1.5 V the time dependence of the current increases dramatically.

As seen in Figure 3b, at high bias voltage the current as function of time resembles an exponential decay towards a steady-state value. The logarithm to the measured decay rates are not obviously linear functions of dissipated power and it is therefore difficult to relate the decay rate to an estimated temperature and corresponding Arrhenius-like dependence of oxidation rate similar to the thermal oxidation experiment by ref 29. We do not observe instantaneous drops in the current as function of time, as reported in experiments on A-MWNTs[1] or small C-MWNTs,[5] since the nanotubes in the present sample contain numerous shells and kinks, where the contribution from rupture of a single shell or merely a section of a shell will only give a minor contribution to the overall electrical behavior of the nanotube.

The onset of decay at the threshold voltage can be taken as an indication of beginning oxidation of the amorphous carbon in the C-MWNT, which should begin at 350 °C. From the dissipated power at the threshold and the nanotube dimensions, the formula $\kappa = LP/(8A\Delta T)$ with $\Delta T = 350$ °C provides an estimate of the thermal conductivity κ for the different tubes. From the measurements we find κ to be in the range 50−200 W/mK, in agreement with previously reported results.[21,22]

5. Discussion. In accordance with observations by other groups, the IV curves of the nanotube devices are nonlinear, with the conductivity increasing with respect to bias voltage lower than 1.5 V. The fixed bias voltage intervals cause the vertical steps at high bias voltage in the IV curves Figure 3a. These steps conveniently indicate how time becomes an increasingly important factor for the shape of the IV curves at high bias voltages. The time dependence should largely account for the saturation behavior of the measured IV curves that is often observed if the bias voltage is continuously increased without temporary stops.

The nonlinearity of the IV curves at low bias voltages, where no time dependence is observed, could be caused by thermal effects in the nanotube bridge. The conductance $G = I/U$ in units of the conductance quantum G_0 vs dissipated power $P = UI$ for the voltage sweeps is surprisingly linear, especially considering the extensive tube damage during each voltage sweep. This indicates a linear dependence on temperature $G_2 = G_1(1 + \beta\Delta T)$ with the temperature proportional to the dissipated power, $\Delta T = (L/(8\kappa A))P$. Combining these equations and expressing them in terms of voltage and current gives a conductivity $I/U = 1/r + cUI$,

with $r = 1/G_1$ and $c = \beta L/(8\kappa A)$, leading to a current−voltage relation $I = U/(r + cU^2)$. The linear conductance-power dependence $G = cP + 1/r$, gives a good fit to the low bias *IV* curve with fitting parameters r and c for each curve, as shown with circles in Figure 3a. For the G vs P curves at high power, the slope is slightly lower and can be explained by oxidation and the accompanying decaying current as function of time. Despite the very extensive damage of the nanotube structure, the sequential Joule heating curves have almost the same slopes for each individual sweep in the G vs P curves (we also find a linear G vs P dependence in our previous results obtained by scanning four point probes on nanotubes in air).[38]

The model of linear temperature dependence of nanotube conductance for the MWNT conduction seems to describe the present sample best, even after several current-induced oxidations of the outer shells have been performed on it, and even when it is nearly broken in two pieces after the second *IV* sweep (see Figure 1).

6. Conclusion and Outlook. The measurements on carbon nanotubes demonstrate the onset of nanotube damage in ambient conditions, with accelerated rate at higher bias voltages. The low bias *IV* curve is reasonably well described by a simple, phenomenological model based on linear dependence of conductivity on temperature and Joule heating. At high bias, the gradual oxidation of the nanotube shells is essential in describing the irreversible conductance change over time. On the basis of the decaying current with respect to time, the oxidation is likely to be the main factor causing the saturation of the *IV* curve for the studied C-MWNT. From the dissipated power at the threshold voltage, where the current begins to decay as function of time, an estimate can be made of the thermal conductivity of the nanotubes, giving reasonable values in the range 50−200 W/mK. Future work comparing different types of multiwalled nanotubes and independent measurements of the dependence of their properties with temperature should be essential for making better models of these interesting nanostructures' properties and evaluating their possible applications in devices.

The presented study also demonstrates the ability to use microcantilever electrodes for combining TEM with other characterization methods to provide unprecedented opportunities for characterizing a pristine individual nanostructure with several techniques. The microfabricated TEM chips (inset in Figure 1) offer good flexibility in terms of varying the design of the cantilevers, facilitating for instance multipoint conductance measurements or even integrated MEMS actuators and sensors for characterization of nano-electromechanical systems. If a nanostructure is suspended between the actuators of a cantilever-based actuator and force sensor[39] or between cantilevers with heaters and microbolometers[40] it should in principle be possible to study the electrical, thermal, and mechanical properties of the pristine nanostructures under a wide range of conditions with the option of performing TEM analysis in situ or between the experiments.

Acknowledgment. We thank Richard Czerw for supplying the nanotube samples.

References

(1) Collins, P. G.; et al. Current saturation and electrical breakdown in multiwalled carbon nanotubes. *Phys. Rev. Lett.* **2001**, *86* (14), 3128−3131.
(2) Nakayama, Y.; Akita, S. Nanoengineering of carbon nanotubes for nanotools. *New J. Phys.* **2003**, *5*.
(3) Poncharal, P.; et al. Room-temperature ballistic conduction in carbon nanotubes. *J. Phys. Chem. B* **2002**, *106* (47), 12104−12118.
(4) Dai, H. J.; Wong, E. W.; Lieber, C. M. Probing electrical transport in nanomaterials: Conductivity of individual carbon nanotubes. *Science* **1996**, *272* (5261), 523−526.
(5) Huang, J. Y.; et al. Atomic-scale imaging of wall-by-wall breakdown and concurrent transport measurements in multiwall carbon nanotubes. *Phys. Rev. Lett.* **2005**, *94* (23).
(6) *Carbon Nanotubes—Synthesis, Structure, Properties and Applications*; Dresselhaus, M. S., Dresselhaus, G., Avouris, P., Eds.; Topics in Applied Physics; Springer-Verlag: New York, 2003; Vol. 80.
(7) Teo, K. B. K.; et al. Uniform patterned growth of carbon nanotubes without surface carbon. *Appl. Phys. Lett.* **2001**, *79* (10), 1534−1536.
(8) Moser, J.; et al. Individual free-standing carbon nanofibers addressable on the 50 nm scale. *J. Vacuum Sci. Technol., B* **2003**, *21* (3), 1004−1007.
(9) Graham, A. P.; et al. Carbon nanotubes for microelectronics? *Small* **2005**, *1* (4), 382−390.
(10) Lee, S. B.; et al. Study of multiwalled carbon nanotube structures fabricated by PMMA suspended dispersion. *Microelectron. Eng.* **2002**, *61−2*, 475−483.
(11) Choi, W. B.; et al. Ultrahigh-density nanotransistors by using selectively grown vertical carbon nanotubes. *Appl. Phys. Lett.* **2001**, *79* (22), 3696−3698.
(12) Yuzvinsky, T. D.; et al. Imaging the life story of nanotube devices. *Appl. Phys. Lett.* **2005**, *87* (8).
(13) Xu, S. Y.; Xu, J.; Tian, M. L. A low cost platform for linking transport properties to the structure of nanomaterials. *Nanotechnology* **2006**, *17* (5), 1470.
(14) Kim, T.; et al. Imaging suspended carbon nanotubes in field-effect transistors configured with microfabricated slits for transmission electron microscopy. *Appl. Phys. Lett.* **2005**, *87* (17).
(15) Chikkannanavar, S. B.; et al. Synthesis of peapods using substrate-grown SWNTs and DWNTs: An enabling step toward peapod devices. *Nano Lett.* **2005**, *5* (1), 151−155.
(16) Meyer, J. C.; et al. Transmission electron microscopy and transistor characteristics of the same carbon nanotube. *Appl. Phys. Lett.* **2004**, *85* (14), 2911−2913.
(17) Kasumov, A. Y.; et al. Conductivity and atomic structure of isolated multiwalled carbon nanotubes. *Europhys. Lett.* **1998**, *43* (1), 89−94.
(18) Lee, S. B.; et al. Characteristics of multiwalled carbon nanotube nanobridges fabricated by poly(methyl methacrylate) suspended dispersion. *J. Vacuum Sci. Technol., B* **2002**, *20* (6), 2773−2776.
(19) Li, Q. H.; Wang, T. H. Shell coupling through a single multiwall carbon nanotube. *Chinese Phys. Lett.* **2003**, *20* (9), 1558−1560.
(20) Purcell, S. T.; et al. Hot nanotubes: Stable heating of individual multiwall carbon nanotubes to 2000 K induced by the field-emission current. *Phys. Rev. Lett.* **2002**, *88* (10).
(21) Yi, W.; et al. Linear specific heat of carbon nanotubes. *Phys. Rev. B* **1999**, *59* (14), R9015−R9018.
(22) Yang, D. J.; et al. Thermal and electrical transport in multiwalled carbon nanotubes. *Phys. Lett. A* **2004**, *329* (3), 207−213.
(23) Blazewicz, S.; Patalita, B.; Touzain, P. Study of piezoresistance effect in carbon fibers. *Carbon* **1997**, *35* (10−11), 1613−1618.
(24) Vincent, P.; et al. Modelization of resistive heating of carbon nanotubes during field emission. *Phys. Rev. B* **2002**, *66* (7).
(25) Zhou, F.; et al. Linear conductance of multiwalled carbon nanotubes at high temperatures. *Solid State Commun.* **2004**, *129* (6), 407−410.
(26) Jang, J. W.; et al. Conduction mechanism of the bamboo-shaped multiwalled carbon nanotubes. *J. Korean Phys. Soc.* **2003**, *42*, S985−S988.
(27) Sekar, C.; Subramanian, C. Purification and characterization of buckminsterfullerene, nanotubes and their byproducts. *Vacuum* **1996**, *47* (11), 1289−1292.
(28) Morishita, K.; Takarada, T. Gasification behavior of carbon nanotubes. *Carbon* **1997**, *35* (7), 977−981.
(29) Lu, X. K.; et al. Scanning electron microscopy study of carbon nanotubes heated at high temperatures in air. *J. Appl. Phys.* **1999**, *86* (1), 186−189.

(30) de Pablo, P. J., et al. Correlating the location of structural defects with the electrical failure of multiwalled carbon nanotubes. *Appl. Phys. Lett.* **1999**, *75* (25), 3941−3943.
(31) Boggild, P.; et al. Fabrication and actuation of customized nanotweezers with a 25 nm gap. *Nanotechnology* **2001**, *12* (3), 331−335.
(32) Andrews, R.; et al. Continuous production of aligned carbon nanotubes: a step closer to commercial realization. *Chem. Phys. Lett.* **1999**, *303* (5−6), 467−474.
(33) Kim, H.; Kaufman, M. J.; Sigmund, W. M. Phase transition of iron inside carbon nanotubes under electron irradiation. *J. Mater. Res.* **2004**, *19* (6), 1835−1839.
(34) Mølhave, K.; Wich, T.; Kortschack, A.; Bøggild, P. Pick-and-place nanomanipulation using microfabricated grippers. *Nanotechnology* **2006**, *17*, 2434−2441.
(35) Svensson, K.; Olin, H.; Olsson, E. Nanopipets for metal transport. *Phys. Rev. Lett.* **2004**, *93* (14).
(36) Matsubara, K.; Sugihara, K.; Tsuzuku, T. Electrical-Resistance in the C-Direction of Graphite. *Phys. Rev. B* **1990**, *41* (2), 969−974.
(37) Shi, L.; et al. Scanning thermal microscopy study of dissipation in current-carrying carbon nanotubes. *Am. Soc. Mech. Eng., Heat Transfer Div., (Publ.) HTD* 2001, *369* (7), 247−252.
(38) Dohn, S.; Molhave, K; Boggild, P. Direct measurement of resistance of multiwalled carbon nanotubes using micro four-point probes. *Sens. Lett.* **2005**, *3* (4), 300−303.
(39) Molhave, K.; Hansen, O. Electro-thermally actuated microgrippers with integrated force-feedback. *J. Micromech. Microeng.* **2005**, *15* (6), 1265−1270.
(40) Shi, L.; Majumdar, A.; McEuen, P. L. Thermal transport measurements of individual multiwalled nanotubes. *Phys. Rev. Lett.* **2001**, APS. 215502/1−4.

NL060821N